COMMISSIONS G1 AND G4 OF THE IAU
INFORMATION BULLETIN ON VARIABLE STARS
Volume 63 Number 6270 DOI: 10.22444/IBVS.6270

Konkoly Observatory
Budapest
3 June 2019

HU ISSN 0374 – 0676

V1097 Her – A W-TYPE OVERCONTACT ECLIPSING BINARY

NELSON, ROBERT H.[1,2]; RUSSELL, ROBB[3]

[1] Mountain Ash Observatory, 1393 Garvin Street, Prince George, BC, Canada, V2M 3Z1
email: bob.nelson@shaw.ca

[2] Guest investigator, Dominion Astrophysical Observatory, Herzberg Institute of Astrophysics, National Research Council of Canada

[3] Department of Physics and Astronomy, University of Victoria, Victoria, BC, Canada
email: robb@uvic.ca

Abstract

V1097 Her, an overcontact (W-type) eclipsing binary, has a short period, a relatively low degree of contact (or fill-out parameter), and an increasing period. It has now been classified: for the more luminous star a spectral type of F8.5V±1 has been determined. B,V,Ic light curves and, for the first time, radial velocity curves for the overcontact binary V1097 Her have been obtained; these have been subjected to a Wilson-Devinney analysis, yielding fundamental parameters; in particular masses of 0.41 ± 0.01 and 1.11 ± 0.02 $M_\odot$ and luminosities of 0.77 ± 0.01 and 1.75 ± 0.03 $L_\odot$ respectively. The distance estimate of $r = 237 \pm 11$ pc is consistent with the Gaia value of $r = 250.3 \pm 1.4$ pc (Bailer-Jones et al., 2018; Gaia Collaboration, 2018). A period analysis, again believed to be the first ever, has been undertaken, revealing a constant rate of period increase of $dP/dt = (1.85 \pm 0.11) \times 10^{-7}$ d/yr.

As a by-product of the ROTSE all-sky survey (Akerlof et al., 2000), well over 1000 new periodic variables were discovered. One of these, V1097 Her (ROTSE1 J173327.94+265547.5, NSVS 8002361, TYC 2083-1870-1) was identified as a EW-type eclipsing binary with a period of 0.360819 d and an amplitude of 0.458 mag (clear filter). Follow-up CCD observations for this system and three others were performed by Bälttler and Diethelm (2002) who obtained new light curves and many new times of minima, one result of which was to refine the period for V1097 Her, obtaining $P = 0.360847$ d (no error estimate). Subsequently, there have been many new published eclipse timings.

An eclipse timing difference (O–C) plot using all the timings from 1999 (earliest) to 2018 is depicted in Fig. 1. Although there is considerable scatter, a quadratic relation over the data collection interval (cycle 28800 to 30770 for the RVs and cycle –3205 to 16047 for the light curve data) was obtained; equation (1) below defines the weighted quadratic fit. (Note: in it, and throughout the paper, figures in brackets denote the error estimates in units of the last digit.)

$$\mathrm{JD\,(Hel)_{MinI}} = 2452463.4068(3) + 0.36084705(1)\mathrm{E} + 8.4(5) \times 10^{-11}\mathrm{E}^2 \qquad (1)$$

A weighted linear least-squares fit for the data from cycle 6881 (2009) to cycle 15129 (2017) yielded the fit of equation (2), used in all phasing.

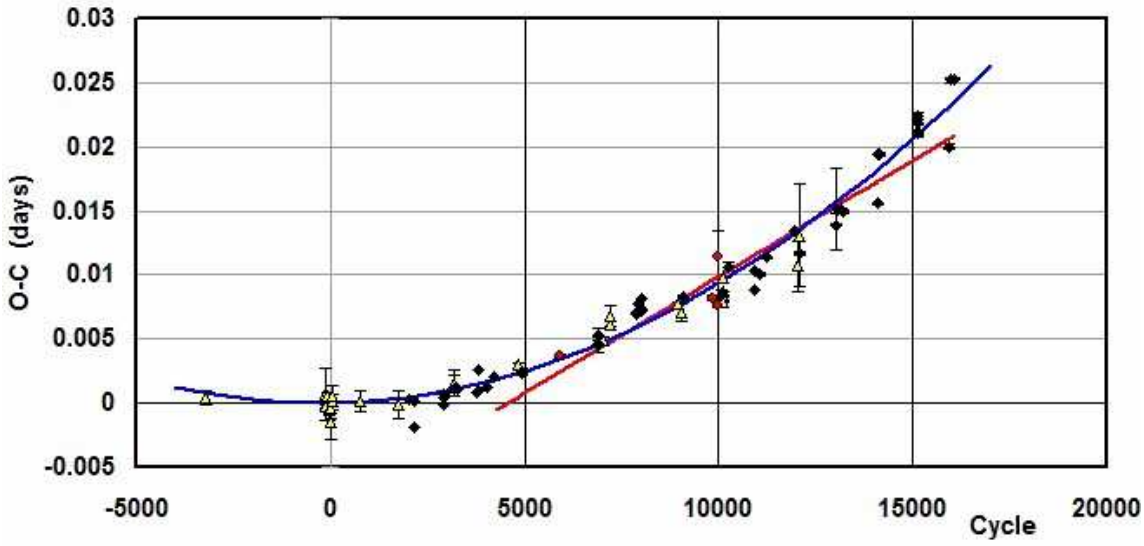

Figure 1. V1097 Her – eclipse timing (O-C) plot with the quadratic fit. Legend: (yellow-filled) triangles - visual, (red) circles - photoelectric, and (black) diamonds - CCD.

$$\mathrm{JD\ (Hel)_{MinI}} = 2458253.9395(10) + 0.3608488(1)\mathrm{E} \qquad (2)$$

The Excel file (and many others) are available at Nelson (2017). The 5000+ files are updated annually. Further eclipse timings are recommended in order to detect, or alternatively rule out a light time effect (LiTE).

There has been no light curve analysis for this system. In order to rectify this lack, the lead author first secured, in April of 2009, 2011, 2015, and 2016 and in September of 2017, a total of 14 medium resolution (R∼10000 on average) spectra of V1097 Her at the Dominion Astrophysical Observatory (DAO) in Victoria, British Columbia, Canada using the Cassegrain spectrograph attached to the 1.85 m Plaskett Telescope. He used the 21181 configuration with the 1800Yb grating (1800 lines/mm, blazed at 5000 Å), which gave a reciprocal linear dispersion of 10 Å/mm in the first order. The wavelengths ranged from 5000 to 5260 Å, approximately. A log of observations is given in Table 1.

Frame reduction was performed by software *RaVeRe* (Nelson 2013). See Nelson (2010a) and Nelson et al. (2014) for further details. The normalized spectra are reproduced in Fig. 2, sorted by phase. Note towards the right the strong neutral iron lines (at 5167.487 and 5171.595 Å) and the strong neutral magnesium triplet (at 5167.33, 5172.68, and 5183.61 Å).

Radial velocities were determined using the Rucinski broadening functions (Rucinski 2004, Nelson 2010a) as implemented in software *Broad25* (Nelson 2013). See Nelson et al. (2014) for further details. An Excel worksheet with built-in macros (written by him) was used to do the necessary radial velocity conversions to geocentric and back to heliocentric values (Nelson 2014). The resulting RV determinations are also presented in Table 1. The mean rms errors for RV1 and RV2 are 8.5 and 7.8 km/s, respectively, and the overall rms deviation from the (sinusoidal) curves of best fit is 8.3 km/s. The best fit yielded the values $K_1 = 250.0(1.5)$ km/s, $K_2 = 87.1(1.5)$ km/s and $V_\gamma = 14.9(1.0)$ km/s, and thus a mass ratio $q_{sp} = K_1/K_2 = M_2/M_1 = 2.87(5)$.

Representative broadening functions, at phases 0.24 and 0.78 are depicted in Figs. 3

Table 1: Log of DAO observations

DAO Image #	Mid Time (HJD-2400000)	Exposure (sec)	Phase at mid-exp	V_1 (km/s)	V_2 (km/s)
09-5354	54927.0236	3378	0.302	–215.1 (8.2)	103.9 (8.6)
09-5396	54928.8629	3600	0.400	—	73.1 (8.1)
09-5425	54929.8849	3600	0.232	–228.1 (7.1)	97.0 (3.2)
11-2578	55670.8957	3600	0.756	258.0 (1.9)	–56.6 (3.0)
11-2675	55674.8901	3600	0.826	225.9 (4.3)	–76.2 (3.9)
15-3150	57121.8629	3600	0.746	270.7 (3.1)	–74.9 (4.2)
16-1288	57493.9341	3600	0.847	245.1 (2.9)	–65.1 (2.6)
16-1328	57495.9094	3600	0.321	–208.2 (3.3)	92.3 (2.0)
16-1358	57496.9657	3000	0.248	–237.5 (3.3)	91.3 (3.0)
17-4017	57859.9463	2500	0.158	–189.7 (1.0)	81.7 (0.2)
17-13704	57997.8196	2500	0.239	–233.8 (1.5)	99.1 (9.3)
17-15737	57998.6748	2500	0.609	—	–32.9 (6.5)
17-15793	57999.8174	2500	0.775	274.5 (10.2)	–71.6 (4.9)
17-15950	58008.8000	2500	0.668	217.8 (2.7)	–67.9 (5.6)

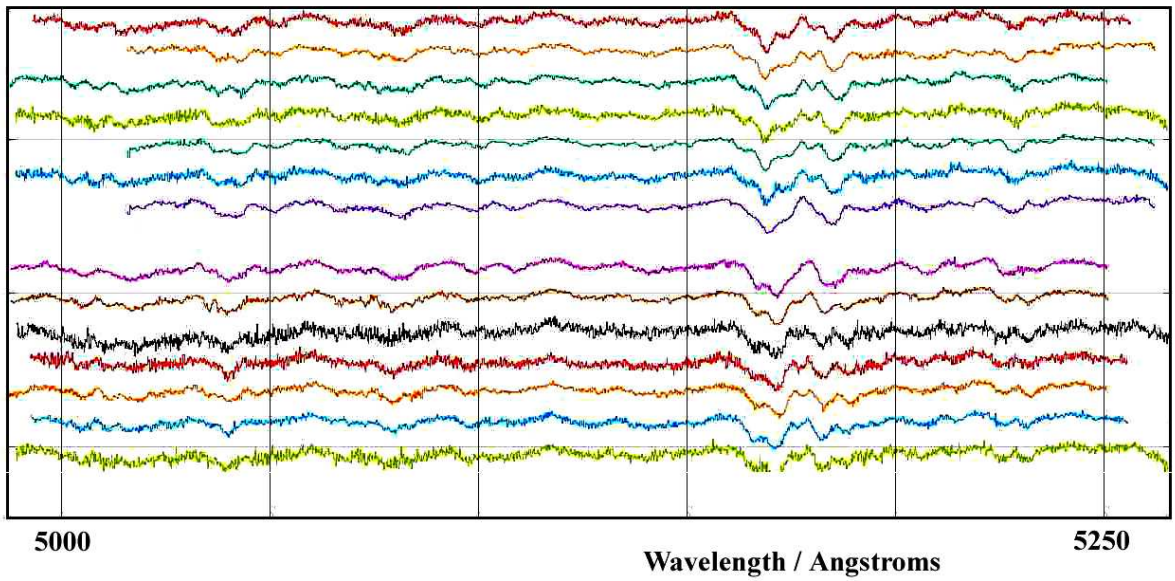

Figure 2. V1097 Her spectra at phases 0.16, 0.23, 0.24, 0.25, 0.30, 0, 32, 0.40, 0.61, 0.67, 0.75, 0.76, 0.78, 0.83, 0.85 (from top to bottom)

and 4, respectively. Smoothing by a Gaussian filter is routinely done in order to centroid the peak values for determining the radial velocities.

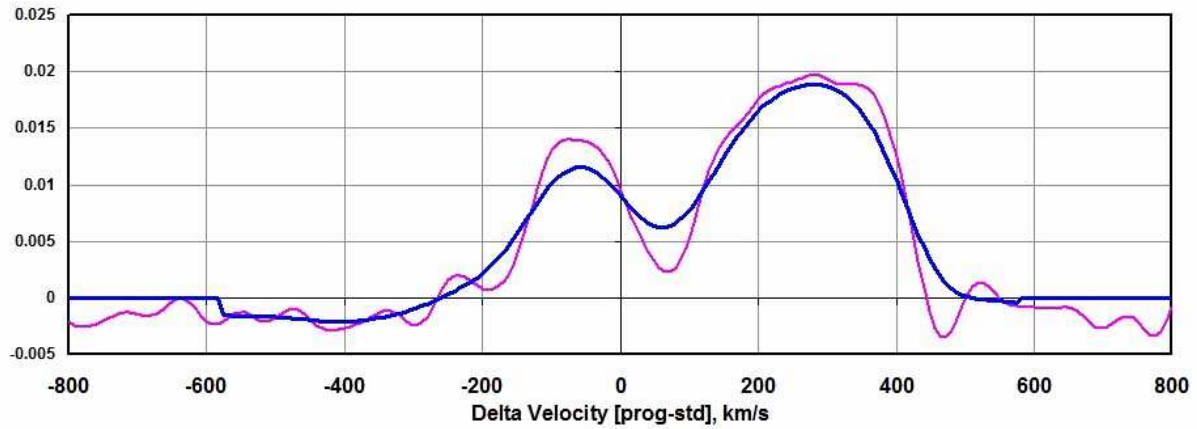

Figure 3. Broadening functions at phase 0.24–smoothed and unsmoothed.

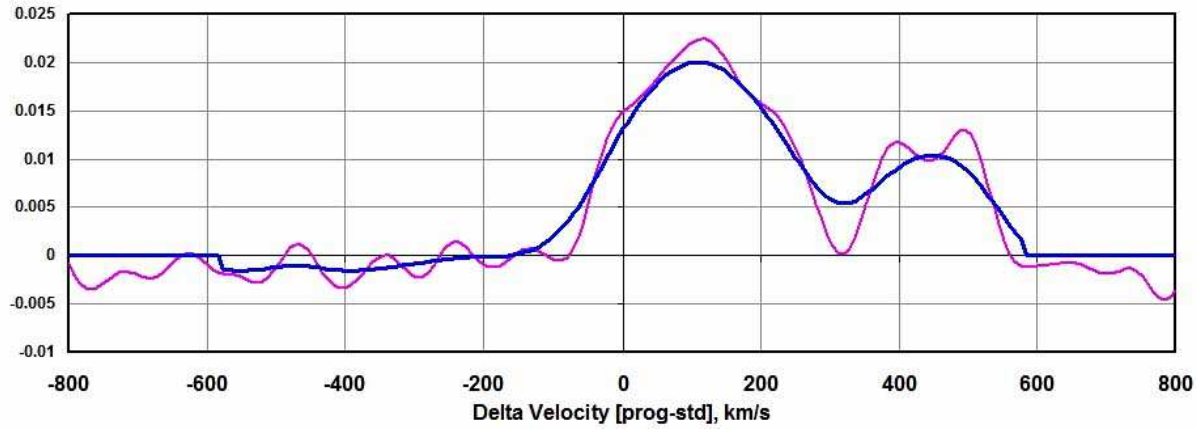

Figure 4. Broadening functions at phase 0.78–smoothed and unsmoothed.

In June of 2011, and again in 2012, the lead author took a total of 87 frames in V, 88 in R_C (Cousins) and 118 in the I_C (Cousins) band at his private observatory in Prince George, BC, Canada. The telescope was a 33 cm f/4.5 Newtonian on a Paramount ME mount; the cameras used were the SBIG ST-7XME and ST-10XME.

Standard reductions were then applied (see Nelson et al., 2014 for more details). The variable, comparison and check stars are listed in Table 2. The coordinates for V1097 Her, the comparison, and check stars (rounded to integral seconds) are from the Tycho Catalogue (Høg et al., 2000), the magnitudes are taken from the AAVSO Photometric All-Sky Survey (APASS, DR9)[1] catalogue (Henden et al., 2012)

The 2003 version of the Wilson-Devinney (WD) light curve and radial velocity analysis program with Kurucz atmospheres (Wilson and Devinney, 1971; Wilson, 1990; Kallrath

[1]https://www.aavso.org/download-apass-data

Table 2: Details of variable, comparison and check stars.

Object	GSC	RA (J2000)	Dec (J2000)	V (mag)	$B-V$ (mag)
Variable	2083-1870	17:33:28	+26:55:47	10.91 (6)	0.58 (10)
Comparison	2083-1693	17:33:37	+26:58:38	10.33 (4)	0.05 (4)
Check	2083-2141	17:33:43	+26:47:56	10.07 (4)	1.49 (7)

and Milone; 1998, Wilson, 1998) as implemented in the Windows front-end software WDwint (Nelson 2013) was used to analyze the data.

For classification purposes, one of the authors (R.M.R.) took two low resolution spectra, on 2013 June 22 (HJD = 2456465.7981; mid exposure, UTC). He used the 1.85 m Plaskett telescope at the Dominion Astrophysical Observatory (DAO) in Victoria, British Columbia, Canada with the Cassegrain spectrograph in the 2131 configuration, resulting in a reciprocal dispersion of 60 Å/mm. The two spectra were very similar (see Fig. 5). The strength of the Calcium H&K lines, G-band, Hγ, Fe I 4384, Ca I 4227, and Hδ lines all indicated a F8.5V±1 spectral classification for V1097 Her.

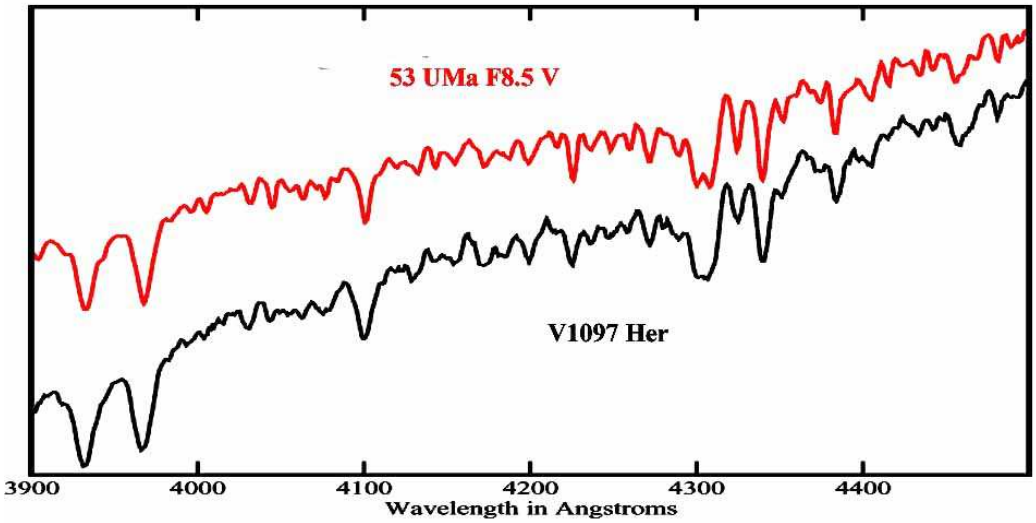

Figure 5. Classification spectra for V1097 Her.

Interpolated tables from Flower (1996) gave a temperature $T_2 = 6191 \pm 162$ K and $\log g = 4.369 \pm 0.006$ (cgs). (The quoted errors refer to one and one half spectral subclass.) An interpolation program by Terrell (1994, available from Nelson 2013) gave the Van Hamme (1993) limb darkening values; and finally, a logarithmic (LD=2) law for the limb darkening coefficients was selected, appropriate for temperatures < 8500 K (ibid.). The limb darkening coefficients are listed below in Table 3. (The values for the second star are based on the later-determined temperature of 6191 K and assumed spectral type of F8.) Convective envelopes for both stars were used, appropriate for cooler stars hence values gravity exponent $g = 0.32$ and albedo $A = 0.5$ were used for each (Lucy, 1967; Rucinski, 1969, respectively).

From the GCVS 4 designation (EW) and from the shape of the light curve, mode 3 (overcontact binary) was used. Later on, mode 2 (detached) was tried. but DC adjust-

Table 3: Limb darkening values from Van Hamme (1993)

Band	x_1	x_2	y_1	y_2
V	0.735	0.739	0.263	0.259
R_C	0.663	0.667	0.274	0.272
I_C	0.579	0.583	0.265	0.264
Bol	0.645	0.644	0.227	0.226

ments required decreases in potential 2 below the critical value, so mode 2 was abandoned.

It was noted immediately that the curve heights at Max I (phase 0.25) and Max II (phase 0.75) were significantly different. This is the O'Connell effect (Davidge & Milone, 1984, and references therein) and is usually explained by the presence of one or more star spots. Accordingly, one was added first to star 2, and this gave good results. (Moving the spot to star 1 gave poorer results and was abandoned.)

Convergence by the method of multiple subsets was reached in a small number of iterations. (The subsets were: (i, q, L_1, R), (T_2, Ω_1), (i, R, Tf), and (i, Lng, R) where i = inclination, q = mass ratio, L_1 = luminosity (scale factor), Ω_1 = potential, Lng = spot longitude, R = spot radius, and Tf = temperature factor). Quantities a (semi-major axis), φ (phase correction), and V_γ (system centre of mass radial velocity) were uncorrelated and therefore could be added to any subset for adjustment.

Detailed reflections were tried, with nref = 3, but there was little–if any–difference in the fit from the simple treatment. There are certain uncertainties in the process (see Csizmadia et al., 2013, Kurucz, 2002). On the other hand, the solution is very weakly dependent on the exact values used.

The model is presented in Table 4. For the most part, the error estimates are those provided by the WD routines and are known to be low; however, it is a common practice to quote these values and we do so here. Also, estimating the uncertainties in temperatures T_1 and T_2 is somewhat problematic. A common practice is to quote the temperature difference over–say–one spectral sub-class. (the case here). In addition, various different calibrations have been made (Cox, 2000, page 388–390 and references therein, and Flower, 1996), and the variations between the various calibrations can be significant. If the classification is ± one sub-class, an uncertainty of ± 150 K to the absolute temperatures of each, would be typical. The modelling error in temperature T_2, relative to T_1, is indicated by the WD output to be much smaller, around 3 K (and is clearly much too low).

The light curve data and the fitted curves are depicted in Figures 6–8. The residuals (in the sense observed-calculated) are also plotted, shifted upwards by 0.55 units.

The Radial Velocities are shown in Fig. 9. A three-dimensional representation from *Binary Maker 3* (Bradstreet, 1993) is shown in Fig. 10 and one for the potentials, in Fig. 11.

The WD output fundamental parameters and errors are listed in Table 5. To save space, those for a similar system, AC Boo (Nelson 2010b), are listed here in column 5-6 and discussed later. Most of the errors are output or derived estimates from the WD routines. From Kallrath & Milone (1998, see also Mochnacki 1981), the fill-out factor is $f = (\Omega_I - \Omega)/(\Omega_I - \Omega_O)$, where Ω is the modified Kopal potential of the system, Ω_I is

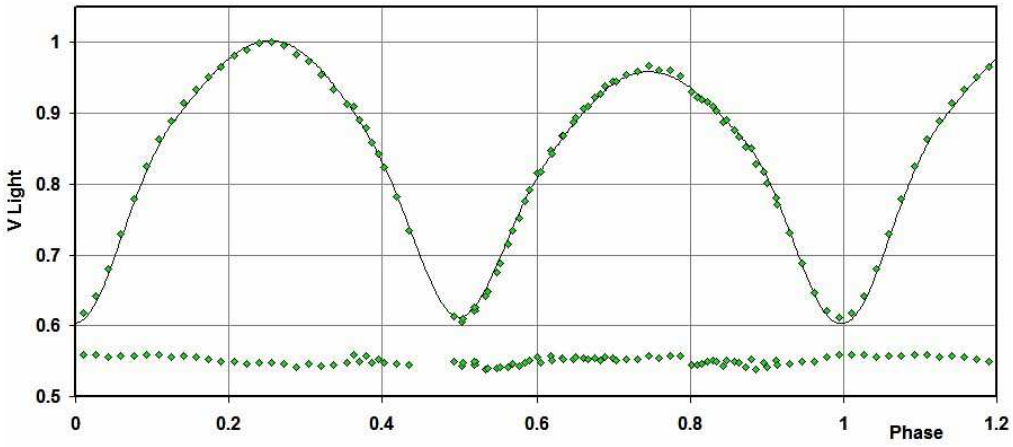

Figure 6. *V* Light Curves for V1097 Her – Data, WD fit, and residuals.

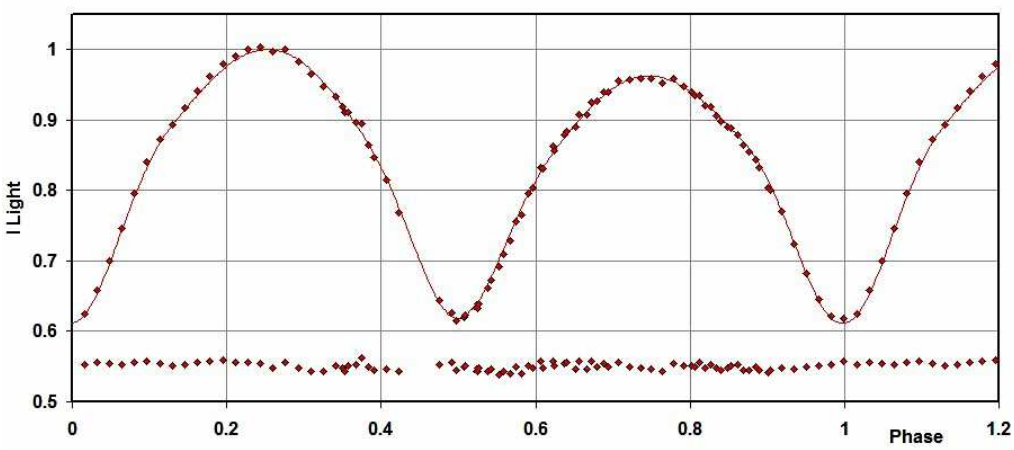

Figure 7. *R* Light Curves for V1097 Her – Data, WD fit, and residuals.

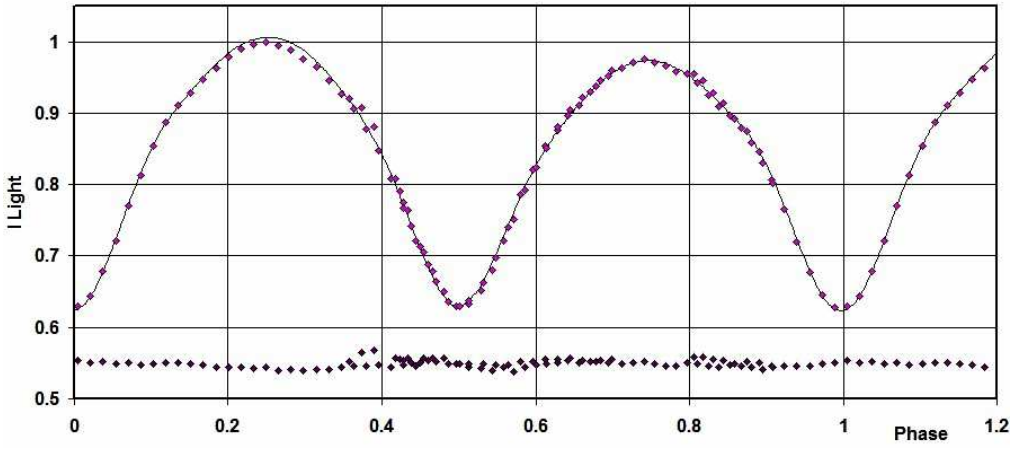

Figure 8. *I* Light Curves for V1097 Her – Data, WD fit, and residuals.

Table 4: Wilson-Devinney parameters

WD Quantity	Value	error	Unit
Temperature, T_1	6250	3	K
Temperature, T_2	6095	[fixed]	K
$q = m_2/m_1$	2.74	0.05	—
Potential, $\Omega_1 = \Omega_2$	6.115	0.007	—
Inclination, i	76.9	0.1	degrees
Semi-maj. axis, a	2.50	0.04	solar radii
V_γ	13.4	1.7	km/s
Phase shift	-0.0030	0.0002	—
Fill-out, f_1	0.13	0.05	
$L_1/(L_1 + L_2)$ (V)	0.312	0.001	—
$L_1/(L_1 + L_2)$ (R_C)	0.309	0.001	—
$L_1/(L_1 + L_2)$ (I_C)	0.305	0.001	—
r_1 (pole)	0.2870	0.0009	orbital radii
r_1 (side)	0.3008	0.0011	orbital radii
r_1 (back)	0.3425	0.0020	orbital radii
r_2 (pole)	0.4507	0.0006	orbital radii
r_2 (side)	0.4849	0.0008	orbital radii
r_2 (back)	0.5152	0.0011	orbital radii
Spot co-latitude	59	10	degrees
Spot longitude	280	3	degrees
Spot radius	21.3	0.5	degrees
Spot temp. factor	0.873	0.002	—
$\Sigma\omega^2_{res}$	0.0285	—	—

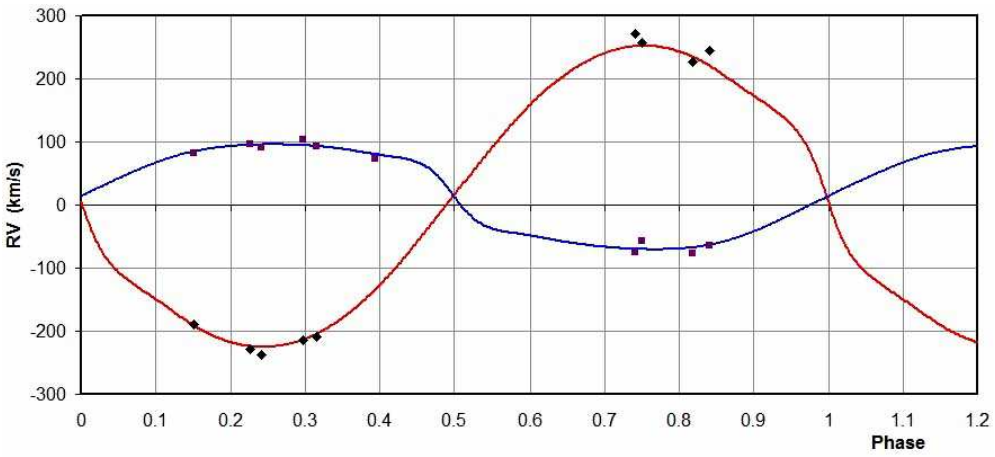

Figure 9. Radial velocity curves for V1097 Her – Data and WD Fit. The primary is represented by (black) diamonds; the secondary, by (purple) squares.

that of the inner Lagrangian surface, and Ω_O, that of the outer Lagrangian surface, was also calculated. In the case of the masses (and mass ratio elsewhere), errors were assigned on the basis of a detailed analysis of errors in the radial velocities (and derived quantities thereof). See Nelson (2015a) for an explanation of the method.

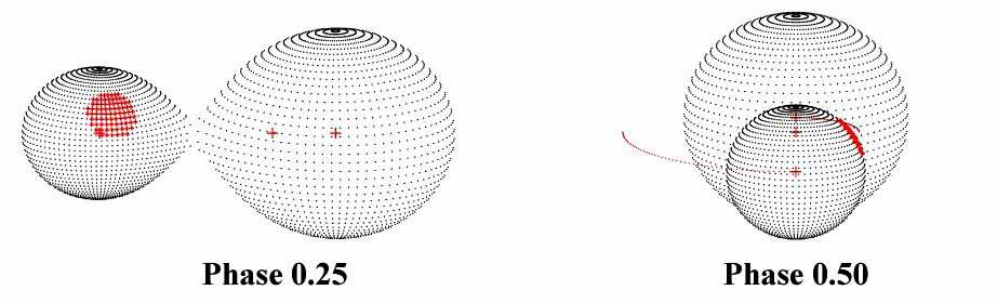

Figure 10. Binary Maker 3 representation of the system – at phases 0.25 and 0.50.

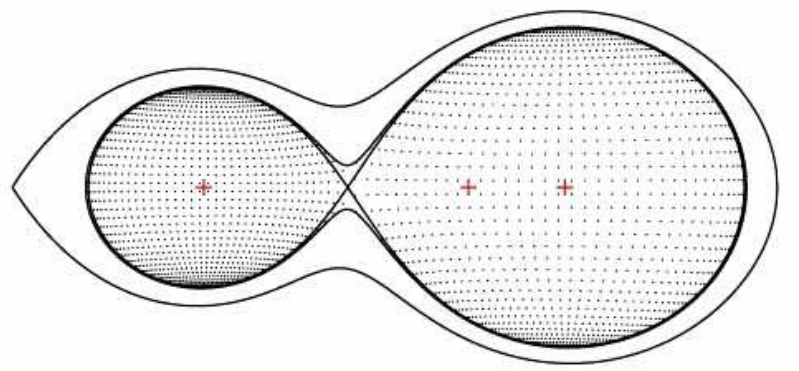

Figure 11. Binary Maker 3 representation of the potentials showing the relatively low degree of contact.

To determine the distance r in column 2, the analysis proceeded as follows: First the WD routine gave the absolute bolometric magnitudes of each component; these were then converted to the absolute visual (V) magnitudes of both, $M_V, 1$ and $M_{V,2}$, by adding the bolometric corrections BC = –0.060 (15) and –0.075 (15) for stars 1 and 2 respectively. The latter were taken from interpolated tables constructed from Cox (2000). The absolute magnitude was then computed in the usual way for adding magnitudes getting $M_V = 3.79 \pm 0.04$ mag. The apparent magnitude in the V passband was $V = 10.91 \pm 0.055$, taken from the APASS Catalogue (Henden et al. 2009, 2010, 2012; Smith et al., 2010).

Ignoring interstellar absorption (i.e., setting $A_V = 0$), we calculated a preliminary value for the distance $r = 265$ pc from the standard relation:

$$r = 10^{0.2(V - M_V - A_V + 5)} \quad \text{pc} \tag{3}$$

Galactic extinction was obtained from a model by Amôres & Lépine (2005). The simple code *extin* (in IDL) assumes that the interstellar dust is well mixed with the dust, that the galaxy is axisymmetric, that the gas density in the disk is a function of the Galactic radius

Table 5: Fundamental parameters of V1097 Her and AC Boo.

Quantity	V1097 Her	Error	unit	AC Boo	Error
Temperature, T_1	6250	150	K	6250	250
Temperature, T_2	6095	150	K	6241	250
Mass, m_1	0.43	0.01	$M_\odot$	0.36	0.03
Mass, m_2	1.19	0.02	$M_\odot$	1.20	0.05
Radius, R_1	0.78	0.02	$R_\odot$	0.69	0.01
Radius, R_2	1.21	0.01	$R_\odot$	1.19	0.01
$M_{bol,1}$	4.98	0.02	mag	5.26	0.02
$M_{bol,2}$	4.13	0.02	mag	4.07	0.02
$\log g_1$	4.29	0.01	cgs	4.32	0.01
$\log g_2$	4.34	0.01	cgs	4.36	0.01
Luminosity, L_1	0.84	0.01	$L_\odot$	0.65	0.09
Luminosity, L_2	1.84	0.03	$L_\odot$	1.94	0.28
Fill-out factor, f	0.13	0.05	—	0.02	
Distance, r	258	8	pc	182	13
Gaia DR2 distance, r	250.3	1.4	pc	156.8	0.6

and of the distance from the Galactic plane, and that extinction is proportional to the column density of the gas, Using Galactic coordinates of $l = 50.5821°$ and $b = 28.11817°$ (SIMBAD), and the initial distance estimate of $d = 0.265$ kpc, a value of $A_V = 0.127$ mag was determined. Further iterations left the value of A_V essentially unchanged. Then, substitution into Eq. (2) yielded a distance of 250 pc.

The same authors provided a more detailed model, *extinspiral* which attempts to take into account the spiral arms of the Galaxy. Starting with an initial distance value $r = 0.265$ kpc as before, we get a somewhat different initial value of $A_V = 0.0609$. Further iterations resulted in no perceptible change in A_V. Then, substitution into Eq. (2) yields a distance of 258 pc.

The errors were assigned as follows: $\delta M_{bol,1} = \delta M_{bol,2} = 0.015$, $\delta BC1 = \delta BC2 = 0.015$ (the variation of 1 and one half spectral sub-classes), $\delta V = 0.055$, all in magnitudes. At this point, it is not clear how to determine the uncertainties in the extinction values A_V from the Amôres & Lépine model. However, if we take half the difference between the two values we get $\delta A_V = 0.03$. Combining the errors rigorously (i.e., by adding the variances) yielded an estimated uncertainty in r of ± 8 pc.

By contrast, reference to the dust tables of Schlegel et al. (1998) revealed a value of $E[B-V] = 0.0474$ for those galactic coordinates, virtually identical with the above values. However, because their $E[B-V]$ values have been derived from full-sky far-infrared measurements, they therefore apply to objects outside of the Galaxy, not the case here. As half the thickness of the Galactic disk is approximately 150 pc (Abell et al., 1991), and the galactic latitude is 28.1° (SIMBAD), that makes the path length $150/\sin(28.1) = 320$ pc. Assuming that the absorption is constant along the path length, we can take $A_V = (237/302) \times 0.145 = 0.113$. Again substituting the value into equation 2 we get $r = 251$ pc, reassuringly not very different from the pervious estimates. Taking δA_V as half of A_V results in an error estimate for r of ± 10 pc.

Another approach, the classical one, is to determine galactic extinction from the tabulated value for the intrinsic $B-V$ colour index and take the difference (observed–tabulated) to get the colour excess $E[B-V]$. So, for a spectral type F8.5, we have (Cox,

Table 6: Estimating the interstellar absorption

Extinction determination	$E[B-V]$ mag	A_V mag	r pc	err pc
Amôres & Lépine (2005) simple model	0.0416	0.1270	250	8
Amôres & Lépine (2005) spiral model	0.0609	0.1857	258	8
Schlegel et al. (1998)	0.0474	0.113	251	10
Classical	0.04	0.122	251	38

2000), $(B-V)_{\rm tables} = 0.54(4)$. From the APASS catalogue we have $(B-V)_{\rm obs} = 0.58(6)$ yielding $E[B-V] = 0.04(7)$ mag. Using the relation $A_V = R\,E[B-V]$ for $R = 3.0$ or 3.1 (we use 3.05 here), we get $A_V = 0.12(34)$ mag and distance $r = 251$ pc, almost identical with the above, but with the higher uncertainty of $\pm\,38$ pc. Especially in view of the large uncertainties in determining $E[B-V]$, it is not surprising that this method results in much larger uncertainties in the final result. It is clear that determining $E[B-V]$ by one of the external methods described above is superior.

We have listed the results in Table 6.

We adopt the weighted mean $r = 253 \pm 5$ pc. However, any of the above distance determinations is consistent with the Gaia distance of 250.3 ± 1.4 pc, which is clearly more reliable.

Conclusion

As mentioned in the abstract, this system has been classified for the first time: the more luminous component has a spectral type of F8.5 V ($\pm\,1$ spectral subclass). Wilson-Devinney light- and radial velocity–curve analysis has determined masses of 0.41(1) and 1.11(2) $M_\odot$ and luminosities of 0.77(1) and 1.75(3) $L_\odot$ respectively. The mass of the secondary (cooler, more massive) star is consistent with the main sequence (interpolated) value of 1.15 $M_\odot$ while the luminosity is higher than the interpolated value of 1.35 $L_\odot$ suggesting a slightly evolved state. On the other hand, the secondary is undermassive for its presumed spectral type (F9, assigned for its temperature) and over-luminous. This is consistent with the model of the evolution of an overcontact system in which the present primary (hotter, less massive) started out as the more massive, losing much of its mass to the present secondary (Yildiz and Doğan, 2013).

This system is surprisingly similar to AC Boo (Nelson 2010b; Alton 2010). In addition to the very similar parameters listed in Table 5, each is type W, each has a spot, in each the more massive star is slightly evolved, and each has a varying orbital period. In the case of AC Boo however, it was shown by Nelson (2015b) that the eclipsing system likely has a companion, and that the more complex period variation may be explained by a light time effect (Irwin 1952, 1959). For AC Boo, the data span some 87 years whereas for V1097 Her, the data span only some 19 years, so one would not expect LiTE behaviour (if it exists) to become evident yet. Further eclipse timings spanning several decades are required to settle the matter. At this stage it is impossible to conclude anything with regard to a possible mass transfer rate because other causes of period change (such as LiTE) have not been ruled out or otherwise accounted for.

Acknowledgements It is a pleasure to thank the staff members at the DAO (Dmitry Monin, David Bohlender, and the late Les Saddlmyer) for their usual splendid help and assistance. Much use was made of the SIMBAD database during this research.

This work has made use of data from the European Space Agency (ESA) mission Gaia (https://www.cosmos.esa.int/gaia), processed by the Gaia Data Processing and Analysis Consortium (DPAC, https://www.cosmos.esa.int/web/gaia/dpac/consortium). Funding for the DPAC has been provided by national institutions, in particular the institutions participating in the Gaia Multilateral Agreement.

References:

Abell, G.O, Morrison, D., and Wolff, S.C., 1991, Exploration of the Universe, (Saunders), p. 539

Akerlof, C., et al., 2000, *AJ*, **119**, 1901

Alton, K. B., 2010, *JAVSO*, **38**, 57

Amôres, E.B., Lépine, J.R.D., 2005, *AJ*, **130**, 659 DOI

Bailer-Jones, C.A.L., et al., 2018, *AJ*, **156**, 58 DOI

Blättler, E. and Diethelm, R., 2002, *IBVS*, 5306

Bradstreet, D. H., 1993, "Binary Maker 2.0 – An Interactive Graphical Tool for Preliminary Light Curve Analysis", in Milone, E.F. (ed.) Light Curve Modelling of Eclipsing Binary Stars, pp 151-166 (Springer, New York, N.Y.) DOI

Cox, A. N., ed., 2000, *Allen's Astrophysical Quantities*, 4th ed., (Springer, New York, NY) DOI

Csizmadia, S., Pasternacki, T., Dreyer, C., Cabrera, A., Erikson, A., Rauer, H., 2013, *A&A*, **549**, A9 DOI

Davidge, T.J., Milone, E.F., 1984, *ApJS*, **55**, 571 DOI

Flower, P. J., 1996, *ApJ*, **469**, 355 DOI

Gaia Collaboration, 2018, *A&A*, **616**, 1 DOI

Henden, A. A., Welch, D. L., Terrell, D., Levine, S. E. 2009, The AAVSO Photometric All-Sky Survey, *AAS*, **214**, 407.02

Henden, A. A., Terrell, D., Welch, D., Smith, T. C. 2010, New Results from the AAVSO Photometric All Sky Survey, *AAS*, **215**, 470.11

Henden, A. A., Levine, S. E., Terrell, D., Smith, T. C., Welch, D., 2012, *JAAVSO*, **40**, 430

Høg, E., et al., 2000 *A&A*, **355**, L27

Irwin, J. B., 1952, *ApJ*, **116**, 211 DOI

Irwin, J. B., 1959, *AJ*, **64**, 149 DOI

Kallrath, J. & Milone, E.F., 1998, *Eclipsing Binary Stars–Modeling and Analysis* (Springer-Verlag) DOI

Kurucz, R.L., 2002, *BaltA*, **11**, 101

Lucy, L.B., 1967, *Zeit. für Astroph.*, **65**, 89

Mochnacki, S. W. 1981, *ApJ*, **245**, 650 DOI

Nelson, R. H., 2010, "Spectroscopy for Eclipsing Binary Analysis" in The Alt-Az Initiative, Telescope Mirror & Instrument Developments (Collins Foundation Press, Santa Margarita, CA), R.M. Genet, J.M. Johnson and V. Wallen (eds) [available on ResearchGate]

Nelson, R.H., 2010b, *IBVS*, 5951

Nelson, R. H., 2013, Software by Bob Nelson, `https://www.variablestarssouth.org/bob-nelson/`

Nelson, R. H., 2014, Spreadsheets, by Bob Nelson, `https://www.variablestarssouth.org/bob-nelson/`

Nelson, R.H., 2015a, *NewA*, **34**, 159 DOI
Nelson, R.H., 2015b, *IBVS*, 6142
Nelson, R.H., 2017, Bob Nelson's O–C Files, http://www.aavso.org/ [enter "O-C" in the search box]
Nelson, R. H., Şenavci, H. V., Baştürk, Ö, Bahar, E., 2014, *NewA*, **29**, 57 DOI
Rucinski, S. M., 1969, *AcA*, **19**, 245
Rucinski, S M., 2004, "Advantages of the Broadening Function (BF) over the Cross-Correlation Function (CCF)", in Stellar Rotation, *IAUS*, **215**, 17
Schlegel, D. J., Finkbeiner, D. P., Davis, M., 1998, *ApJ*, **500**, 525 DOI
Smith, T. C., Henden, A., Terrell, D., 2010, AAVSO Photometric All-Sky Survey Implementation at the Dark Ridge Observatory, SAS.
Terrell, D., 1994, Van Hamme Limb Darkening Tables, vers. 1.1.
Van Hamme, W., 1993, *AJ*, **106**, 2096 DOI
Wilson, R. E., Devinney, E. J., 1971, *ApJ*, **166**, 605 DOI
Wilson, R. E., 1990, *ApJ*, **356**, 613 DOI
Wilson, R. E., 1998, Documentation of Eclipsing Binary Computer Model (available from the author)
Yildiz, M., Doğan, T., 2013, *MNRAS*, **430**, 2029 DOI